CONF-900149--2

UCRL- 102017
PREPRINT

UCRL--102017

DE90 008307

Reactive Sputtering of Molybdenum

A. F. Jankowski
L. R. Schrawyer

This paper was prepared for submittal to the Conference Proceedings for the 8th International Conference on Thin Films: ICTF-8; 17th International Conference on Metallurgical Coatings: ICMC-17, San Diego, CA., April 2-6, 1990.

January 1990

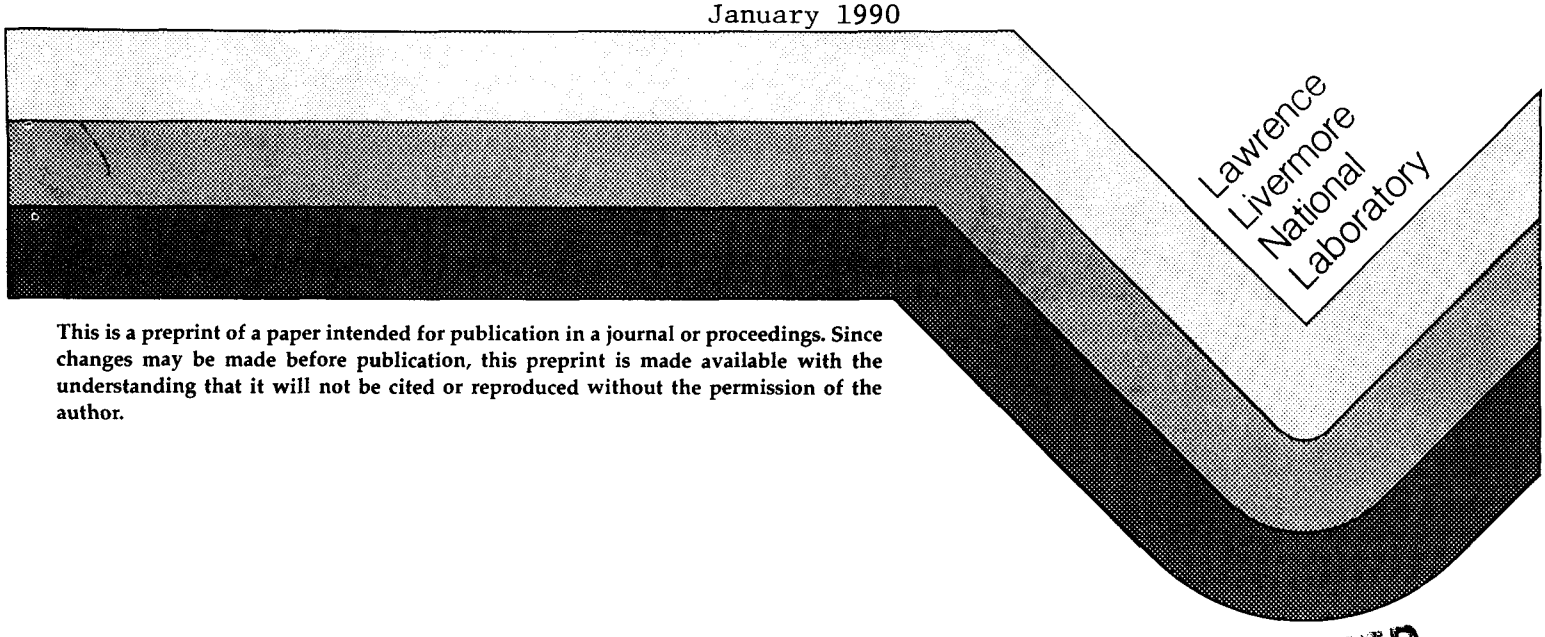

DISCLAIMER

Reactive Sputtering of Molybdenum

A. F. Jankowski and L. R. Schrawyer

Lawrence Livermore National Laboratory
Livermore, California 94550

Abstract

The composition and crystalline structure of molybdenum-oxide thin films is controlled through the process of reactive dc magnetron sputtering. A systematic variation in target power density results in a continuous transition in the appearance of molybdenum-oxide from a translucent glass to a metallic-like film. New molybdenum-oxide crystal structures and compositions are found using XRD, SAD, AES depth profiling and STEM.

1. Introduction

The optical, electrical, magnetic and physical properties of metallic oxide thin films are of increasing technological importance.[1-4] Areas of interest and application include improved ductility, band pass filters and electronic interconnects. Reactive sputtering offers the advantages of forming many complex compounds and insulating materials using dc power supplies and metallic target materials. Reactions between the sputtering gas and target can occur at the surface of the target, at the substrate and in the gas (vapor) phase.

The use of a reactive-gas/argon gas mixture, as in this study, produces films whose properties and composition vary nonlinearly with the reactive gas partial pressure and flow. It is therefore desirable to control the deposited film stoichiometry in a continuous, reproducible manner. Perhaps the simplest process parameter to vary, for this purpose, is the target power density. It is proposed that by singulary varying the applied power (Watts), the corresponding composition of the forming metallic-oxide will continuously vary. (The gas composition and flow rate are concurrently held constant.) The Mo-O system, is one in which a continuous series of crystalline compounds may be expected.[5] This system is therefore well suited for this approach and will be investigated in this study.

2. Reactive Sputter Deposition

The process of reactive dc planar magnetron sputtering is used to produce a series of 1.4-2.7 μm thick molybdenum-oxide films. A .99994 pure Mo metal

target (6.35 cm diameter x 0.635 cm thick) is sputtered using an Ar-20% O_2 gas mixture following a high vacuum bake out at 250°C for 4 hours. The substrates [which include (111) Si wafers, cleaved muscovite and polished glass slides] are positioned 8.9 cm away from the deposition source. The substrates are clamped to an aluminum platen which is shuttered during the ramp to full power. The sputter deposition is started after the substrate temperature has cooled below 100°C, at which point the (cryogenically pumped) chamber base pressure is less than $1x10^{-7}$ Torr. The temperature of the substrate for all depositions ranged from 60 to 85°C. In this context, it may be viewed as a constant substrate temperature. A working gas pressure of 5 mTorr is then applied for all deposition runs using a flow rate of 21.5 sccm/min.

The composition of the molybdenum-oxide films is sought to be continuously and reproducibly controlled with the power supplied to the magnetron source. The gas mixture, pressure and flow remain fixed for all depositions. The change in target power which ranged from 75 to 200 Watts in these experiments, is accompanied by change in the applied potential (voltage) as well as deposition rate. The deposition rates are calculated by dividing the coating time into the measured thickness. These values are equivalent to instantaneous INFICON crystal monitor readouts. A possible discontinuity appears in the deposition rate (of Fig. 1) between 105-110 Watts. The series of high through low power depositions are repeated, in random order, to ensure experimental reproducibly. The decrease in target voltage with increase in supplied power suggests a transition in the nature of the deposition process from that of dielectric to fully conducting metallic. Thus, the increase in current exceeds the rate of increase in supplied power, and is followed by a rapid increase in deposition rate (as seen in Fig. 1). For comparison,

initial sputtering of the molybdenum target with pure Ar produces a 0.37 nm/s deposition rate using 100 Watts and 267 Volts. Whereas the deposition rate at 100 Watts using pure Ar is equivalent to that of the reactive gas mixture, similar target voltages are produced for Ar-20%O_2 gas sputtering near and above ~150 Watts.

3. Composition Determination

3.1 Auger Electron Spectroscopy (AES)

Atomic concentration profiles of the molybdenum-oxide thin films are measured using AES depth profiling. A 3 KeV, 10 μA electron beam is used to generate the Auger electrons. The measured intensities of the 186 eV molybdenum peak, the 272 eV carbon peak and the 503 eV oxygen peak from data accumulated in the derivative mode are used to compute the atomic concentrations. A 5 keV, 2.2 μA argon ion beam is used to sputter etch a 25 mm^2 area of the sample surface. The gas pressure for the sputter etch is $3x10^{-5}$ Torr whereas the system base pressure was below $5x10^{-10}$ Torr. An example of a typical AES depth profile, in this case for a 150 Watt deposit, is shown in Fig. 2. The contamination of the surface with carbon is quickly removed during the depth profile, as the Mo and O concentrations stabilize and remain constant thereafter. Background values for the Si substrate (detected using the 92 eV peak) and C remained below 2 at pct.

The AES depth profile results for those samples measured are summarized in the data points of Fig. 3. AES data for samples reactively deposited below 100 Watts are unavailable. These samples periodically discharge, producing an unreliable quantitative interpretation.

3.2 Scanning Transmission Electron Microscopy (STEM)

In addition to oxide films deposited on Si wafers and used for the AES quantitative analysis, films of the same deposition runs are floated off companion mica substrates and used for STEM microanalysis. The semi-quantitative analysis of ion-milled molybdenum-oxide films in the STEM mode is performed using an energy dispersive spectrometer (EDS). The intensities of characteristic x-ray energies from the oxygen K and molybdenum L lines are used to determine the composition of the foil. The molybdenum-oxide foils are assumed to be 100 nm thick and have a 5 gm/cc density in the area being probed with the electron beam. An example of the spectrum generated, for a 120 Watt deposit, is shown in Fig. 4. The data used in the microanalysis of each sample was accumulated for 200-300 seconds. Variations less than 3 at.pct. resulted from measurements at different positions on the same foil.

The molybdenum concentration variation with target power (Watts) of the reactively sputtered deposits is nearly linear. Both AES depth profile and STEM data reveal similar values for a continuous increase in molybdenum concentration with increased target power.

4. Crystalline State

The use of electron and x-ray diffraction provides the basis on which to characterize the state of crystallinity of the reactively sputtered molybdenum-oxide films.

4.1 X-Ray Diffraction (XRD)

The films are initially characterized in an ordinary powder diffractometer, operated in the $\theta/2\theta$ mode, using a graphite monochromator and CuK_α (0.1542 nm wavelength) radiation. A variation in state of crystallinity with each type of substrate is immediately evident.

Molybdenum-oxide films deposited on the mica substrates are crystalline. In fact, the reactively sputtered films appear to grow epitaxial to the single crystal mica substrates. Both MoO_2 and MoO_3 crystalline compounds have coincident reflections with Muscovite-2M1. To distinguish the crystalline reflections of the coatings from the mica substrate, a 2° tilt (of the sample) added to the angle θ proved sufficient to steer the mica reflections outside the detector receiving slit. This was determined satisfactory, after testing this method on a 1.6 μm thick pure molybdenum foil sputter deposited onto the mica using pure argon as the working gas. The results of applying the tilting procedure successfully remove all superimposing mica reflections (Fig. 5b) from the coating reflections (Fig. 5a). The molybdenum-oxide planar spacings measured are listed in Table I.

The molybdenum-oxide films deposited between 75 and 90 Watts most closely match the orthorhombic form of MoO_3 with peaks nearly matching the (006) and (0010) mica reflections. This stoichiometry corresponds to that suggested by the data of Fig. 3. For the 95 watt deposit, an additional near match to the (0016) mica reflection appears with a slight increase in the (021) MoO_3 spacing. Between 100 and 110 watts the deposit peak reflections coincide with the (0010), (006), (008), (004) and (0016) mica spacings almost exactly (i.e. less than 0.002 nm differences). At 115 watts (Fig. 6a), only the (008) and (0014) mica like reflections are present. These reflections also match the

(200) and ($\bar{4}$02) reflections for the monoclinic form of MoO_2. These two reflections remain for the 120 watt deposit as well. At 125 watts only the (008) mica-like reflection of (200) MoO_2 remains. At 175 watts the remnant (200) peak has broadened considerably (to a full width at half maximum of 3°), possibly incorporating the (111) and ($\bar{2}$11) peaks of MoO_2 as well. At 200 watts, mica-like (008), (0014) and (0016) reflections appear with the most intense being at an additional peak whose spacing coincided to .208 nm. The only molybdenum compounds with a .208 nm planer spacing are either cubic MoOC or Mo_2C. The AES depth profile analysis has revealed a trace amount of carbon (<2 at.pct.) but not enough for these compounds. It may be possible that a new crystalline Mo_2O compound has formed.

After performing the 2° tilt experiments, those molybdenum-oxide films which could be floated off the mica substrates in a water bath (those of metallic character deposited above 100 watts) are dried onto glass slides then re-examined without a 2° tilt. With less than a 0.003 nm shift in peak positions the $\theta/2\theta$ scans of the 2° tilt condition are duplicated, as for the 115 watt deposit (Fig. 6b). The results confirm the validity of the XRD findings for the adherent metallic-oxide glasses deposited on mica below 100 Watts.

In contrast to the results obtained for mica substrates, the deposits characterized on the Si wafers and glass slides are not always crystalline. From 75 to 100 watts, an amorphous deposit is suspected as no well defined crystalline reflections are present (Fig. 7a). At 105 watts, diffuse peaks corresponding to an amorphous form of the MoO_3 phase appear. At 110 Watts, the (200), ($\bar{2}$22) and ($\bar{4}$02) peaks of monoclinic MoO_2 are present (Fig. 7b). From 115 to 120 watts, the texturing of the films shifts to the ($\bar{2}$20) monoclinic MoO_2 reflection. At 125 watts the texturing shifts to the (200)

monoclinic MoO_2 peak, becoming less intense (more diffuse) at 150 watts. Beyond 175 watts, the cubic MoOC peaks become present (as for those deposits on mica) with enhanced texturing of the (200) reflection present at 200 watts (Fig. 7c).

4.2 Transmission Electron Microscopy (TEM)

The crystallinity of the deposits are studied using selected area diffraction (SAD) along with bright-field (BF) and dark-field (DF) imaging. The foils are initially floated from the mica substrates in a water bath, dried flat, then subsequently ion-milled to thin the sample sufficiently for viewing in plan-section.

Those samples which are characterized as amorphous using XRD are confirmed as amorphous using TEM. The bright- and dark-field images of the 150 watt deposit show no signs of diffraction contrast (as seen in Fig. 8a and 8b). The corresponding SAD shows only the broad halo of the amorphous phase (Fig. 8c).

The deposits for which XRD indicates crystallinity, the corresponding TEM analysis typically reveals a composite structure of sub-micron crystals within an amorphous matrix as seen in the BF image (Fig. 9a) for a 125 Watt deposit. The SAD pattern from the matrix (Fig. 9b) confirms its amorphous state whereas the simplest interpretation available from the SAD patterns of the crystallite indicates hexagonal closed packing (hcp). The SAD pattern (Fig. 9c) about the $[2\bar{1}\bar{1}0]$ zone axis, with double diffraction apparent at the (0001) and $(000\bar{1})$ positions, is found. After tilting 90° about $[01\bar{1}0]$, the SAD pattern about the [2423] pole is generated (Fig. 9d). The planar spacings measured from the SAD pattern (of Fig. 9c) are .2488, .1783, .1244 nm, etc. coincide with the

XRD values. The crystal system identification, however, is more thorough using SAD and will be necessary to properly characterize the crystal systems of all the molybdenum-oxide deposits.

5. Discussion of Results

Many process models and experiments of reactive sputtering emphasize the reactive gas partial pressure and flow rate.[6-13] It has been suggested by Hollands and Campbell[7] that a critical O_2 pressure exists, above which reaction at the substrate is transferred to reaction at the target. For the partial pressure and flow rate of O_2 used in the current molybdenum-oxide deposition experiments, it may be inferred from calculations made by Abe and Yamashina[9] that the sputtering rate of the target material is equivalent to that of the pure metal. Therefore, reaction at the substrate is promoted and controlled through the experimental range of applied target power. This prediction is in agreement with the sputtering rate generated at 100 watts being equivalent for pure Ar and the reactive gas mixture, suggesting no significant target surface reaction. The increase of molybdenum content in the oxide deposit coincides with increase in the power supplied to the sputtering target (and consequent increase in deposition rate). This indicates that the Mo-O reaction rate is surpassed by the increased arrival rate of the sputtered species at the substrate.

The control of the molybdenum-oxide reaction/rate at the substrate has permitted the formation of a composition continuous series of molybdenum-oxides. Although the molybdenum-oxygen composition appears to continuously vary, the formation of metastable amorphous/crystalline structures does result. Off-stoichiometric structures of known oxide phases

are possible (as MoO_2 and MoO_3) as well as epitaxially grown deposits (on mica). It is obvious that these crystalline states are not the only ones possible. For example, AES and XRD analysis of the 175 and 200 Watt deposits suggest a new cubic Mo_2O phase, whereas TEM (SAD) and AES analysis of the 125 Watt deposit indicate a new hcp $Mo_{.45}O_{.55}$ phase. Conventional XRD pattern identification alone (as indicated by the best matches with known JCPDS files listed in Table I) may be inadequate. Deposition conditions, as elevated substrate temperature, may lead to other metastable structures.

The existence of such a series of composition dependent molybdenum-oxide crystal structures is quite feasible. For example, it may be that within the order-disorder framework of a bcc host-lattice, extending from the amorphous state, that the crystalline oxides identified in these experiments occur. Khachaturyan[5] suggests that the atomic structures of homologous (Magneli) phases as Ti_nO_{2n-1} are long-period interstitial layer superstructures in the bcc host oxygen lattice. (The existence of the fcc based Mo_nO_{3n-1} is predicted[5] and known experimentally.[14]) The concentration wave approach[5] has been used[15] to predict the atomic arrangement of both octahedral and tetrahedral interstitials in (bcc) molybdenum ordered solutions. The formation of such new phases is possible (and may have formed) by the non-equilibrium nature of the sputtering process itself.

6. Concluding Remarks

Crystalline and amorphous phases of molybdenum-oxide are reactively sputter deposited with stoichiometries continuously ranging from $Mo-O_3$ through Mo_2O. The observation of many non-stoichiometric compounds, suggests interstitial occupancies within a host lattice framework. The

characterization of the composition has been relatively straightforward using AES and STEM. Further characterization of the crystalline structure, coupling XRD and SAD, is required to fully understand the crystalline changes which accompany the molybdenum-oxygen composition variation. For example, in addition to well known MoO_2 and MoO_3 crystalline structures, the possible formation of new Mo_2O cubic and MoO hexagonal based-crystals have occurred during reactive sputtering.

The formation of a composition continuous series of molybdenum-oxide structures may be technologically useful in optics as well as microelectronics. The key process parameter by which these molybdenum-oxide deposits are formed is the target power density. Under constant conditions in which the substrate temperature is low (<80°C) and the Ar-20% O_2 sputtering gas mixture (with respect to a 1 mTorr partial pressure and 4.3 sccm/min flow of the reactive gas component, O_2) is manipulated to favor reaction at the substrate, the continuous variation in applied target power proves useful to reproducibly control the composition and substrate dependent crystalline structure of the forming molybdenum-oxide deposit.

Acknowledgments

The following individuals are thanked for their contribution to the contents of this work - Prof. Armen Khachaturyan (insightful discussions), M. Wall (STEM and SAD analysis of free-standing foils), L. Summers (XRD scans). Work performed under the auspices of the U.S. Department of Energy by Lawrence Livermore National Laboratory under contract #W-7405-Eng-48.

999Q/jg

References

1. R. G. Frieser, J. Electrochem. Soc. 113, (1966) 357.
2. W. W. Molzen, J. Vac. Sci. Technol. 12, (1975) 99.
3. S. F. Vogel and I. C. Barlow, J. Vac. Sci. Technol. 10, (1973) 381.
4. K. A. Müller and J. G. Bednorz, Science 237, (1987) 1133.
5. A. G. Khachaturyan and B. I. Pokrovskii, Prog. Mater. Sci. 29, (1985) 1.
6. S. Berg, H.-O. Blom, M. Moradi, C. Nender and T. Larsson, J. Vac. Sci. Technol. A 7, (1989) 1225.
7. E. Hollands and D. S. Campbell, J. Mater. Sci. 3, (1968) 544.
8. K. Steenbeck, E. Steinbeib and K.-D. Ufert, Thin Solid Films 92, (1982) 371.
9. T. Abe and T. Yamashina, Thin Solid Films 30, (1975) 19.
10. L. F. Donaghey and K. G. Geraghty, Thin Solid Films 38, (1976) 271.
11. F. Shinoki and A. Itoh, J. Appl. Phys. 46, (1975) 3381.
12. S. Maniv and W. D. Westwood, J. Appl. Phys. 51, (1980) 718.
13. E. Bjornard, SPIE Vol. 1019 Thin Film Technologies III, (1989) 24.
14. Problems of Nonstoichiometry, ed. A. Rabenau (North-Holland, Amsterdam, 1970).
15. A. F. Jankowski, "The Theory of Order-Disorder Transitions to Predict the Atomic Arrangement of Interstitials in Molybdenum Ordered Solution" (1982) to be published.

TABLE 1. XRD Data of Moly-Oxide Sputter Deposits

Power (Watts)	Substrate	n^{th} Peak Intensity Planar Spacings (nm) 1st	2nd	3rd	4th	5th	JCPDS best fits
75	mica/2°tilt	.32480	.19699	-	-	-	orthorh MoO_3
75	(111) Si	.352(3°)	.174(6°)	-	-	-	amorph MoO_3
90	mica/2°tilt	.32713	.19682	-	-	-	orthorh MoO_3
95	mica/2°tilt	.32898	.19715	.12358	-	-	orthorh MoO_3
95	(111)Si	.350(3°)	.175(6°)	-	-	-	amorph MoO_3
100	mica/2°tilt	.19744	.32616	.12396	.24607	.14151	mica-MoO_3
105	mica/2°tilt	.19666	.12379	.14121	.32477	.16440	mica-MoO_3
105	(111)Si	.351(3°)	.266(3°)	.173(7°)	-	-	amorph MoO_3
110	mica/2°tilt	.33191	.19930	.24904	.49760	.12451	mica-MoO_3
110	(111)Si	.24585	.17049	.14189	.21812	-	monocl MoO_2
115	mica/2°tilt	.24533	.14128	-	-	-	monocl MoO_2
115	(111)Si	.17228	.34508	.24637	.14204	.12240	monocl MoO_2
120	mica/2°tilt	.24151	.14623	-	-	-	monocl MoO_2
120	(111)Si	.17264	.34557	.14174	.24611	.12235	monocl MoO_2
125	mica/2°tilt	.24456	-	-	-	-	monocl MoO_2
125	(111)Si	.24507	.14121	.12246	-	-	monocl MoO_2
150	(111)Si	.251(3°)	.195(6°)	.149(6°)	-	-	amorph MoO_2
175	mica/2°tilt	.243(3°)	-	-	-	-	amorph MoO_2
175	(111)Si	.20815	.24026	.14701	.12534	.12019	cubic MoOC
200	(111)Si	.20797	.24026	.12545	.14709	.10398	cubic MoOC

Note: Full widths at half maximum values are listed in parenthesis

Figure Captions

Fig. 1 The variation in deposition rate (nm/s) and voltage with applied power (watts) is plotted for the reactive sputtering of pure Mo with an Ar-20% O_2 gas mixture at 5 mTorr and 21.5 sccm/min.

Fig. 2 The molybdenum and oxygen contents of the reactively sputtered deposit are uniform through the film thickness as revealed in this AES depth profile of a 150 Watt deposit.

Fig. 3 The variation in molybdenum concentration with power (Watts) is nearly linear for reactively sputtered films using a Ar-20% O_2 gas mixture. The results obtained using AES depth profiles and STEM.

Fig. 4 STEM Mode generated EDS data accumulated during 347 sec. from the matrix of a 120 Watt reactively sputtered deposit of Mo-O. The film is assumed to be 100 nm thick and have a 5 gm/cc density at the region probed.

Fig. 5 CuKα $\theta/2\theta$ XRD scans of pure Mo on mica substrates (a) tilted an additional 2° to eliminate (b) superimposing substrate reflections.

Fig. 6 CuKα $\theta/2\theta$ XRD scans of the 115 Watt Mo-O deposit on (a) mica, and then floated off the mica and examined on (b) a glass slide. A tentative identification is monoclinic MoO_2.

Fig. 7 CuKα θ/2θ XRD scans of the Mo-O deposits on (111)Si sputtered at (a) 75 Watts (amorphous), (b) 110 Watts (monoclinic MoO_2) and (a) 200 Watts (a new cubic Mo_2O phase?).

Fig. 8 TEM analysis of the 150 Watt Mo-O deposit indicates the structure is amorphous as seen in (a) BF, (b) DF and (c) SAD.

Fig. 9 TEM analysis of the 125 Watt Mo-O deposit indicates the structure is composed of (a) cystallites (BF image) in (b) an amorphous matrix (SAD). The crystallites are most likely hcp as indicated by the SAD patterns about the (c) $[2\bar{1}\bar{1}0]$ pole and after tilting 90°, the (d) $[\bar{2}4\bar{2}3]$ pole.

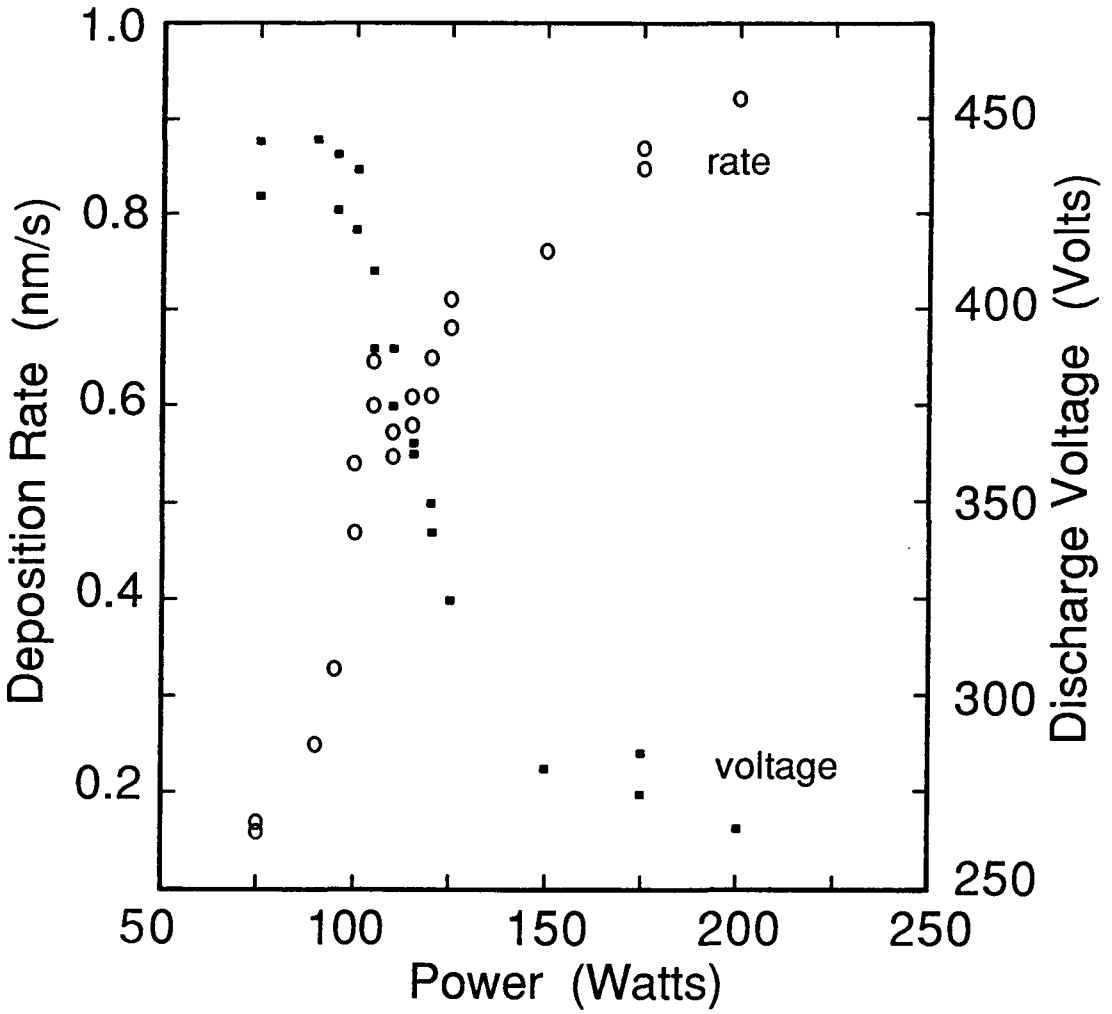
1.0
0.8
0.6
0.4
0.2
Deposition Rate (nm/s)
450
400
350
300
250
Discharge Voltage (Volts)
rate
voltage
50
100
150
200
250
Power (Watts)

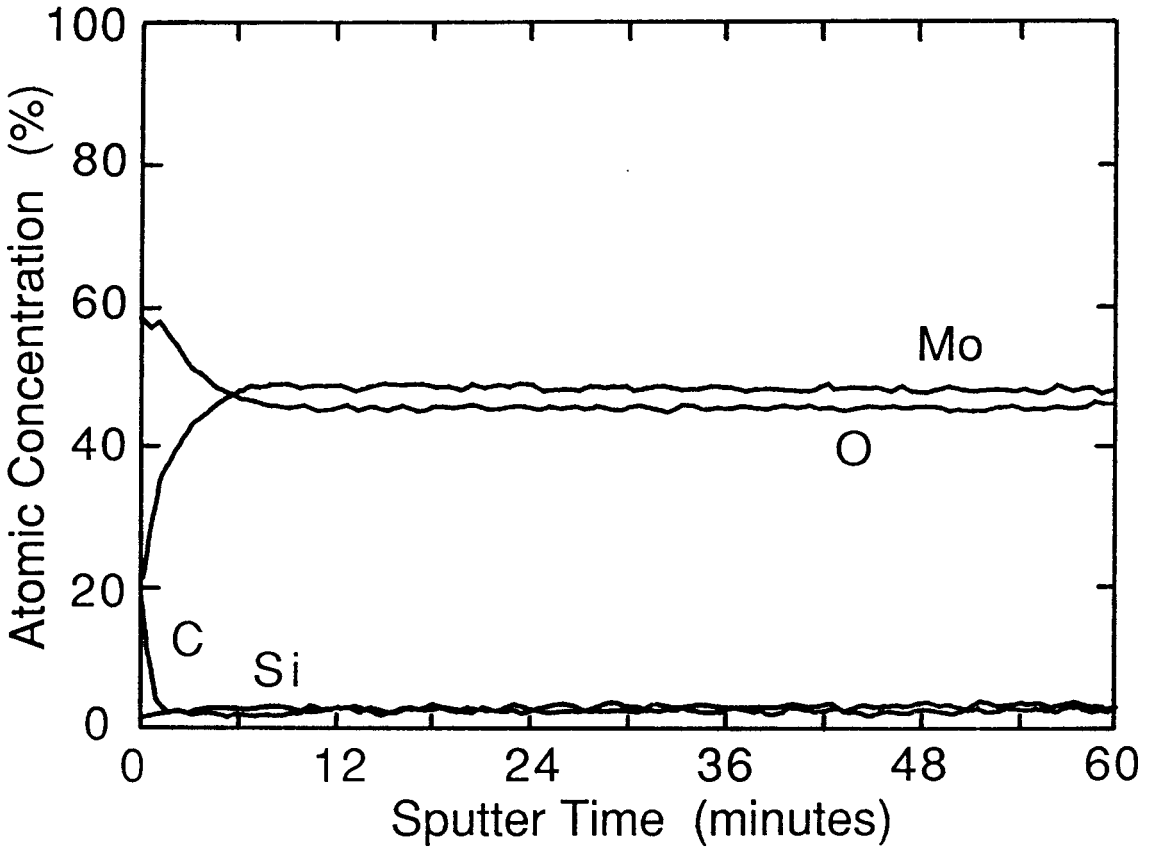
100
80
60
40
20
0
Atomic Concentration (%)
Mo
O
C
Si
0
12
24
36
48
60
Sputter Time (minutes)

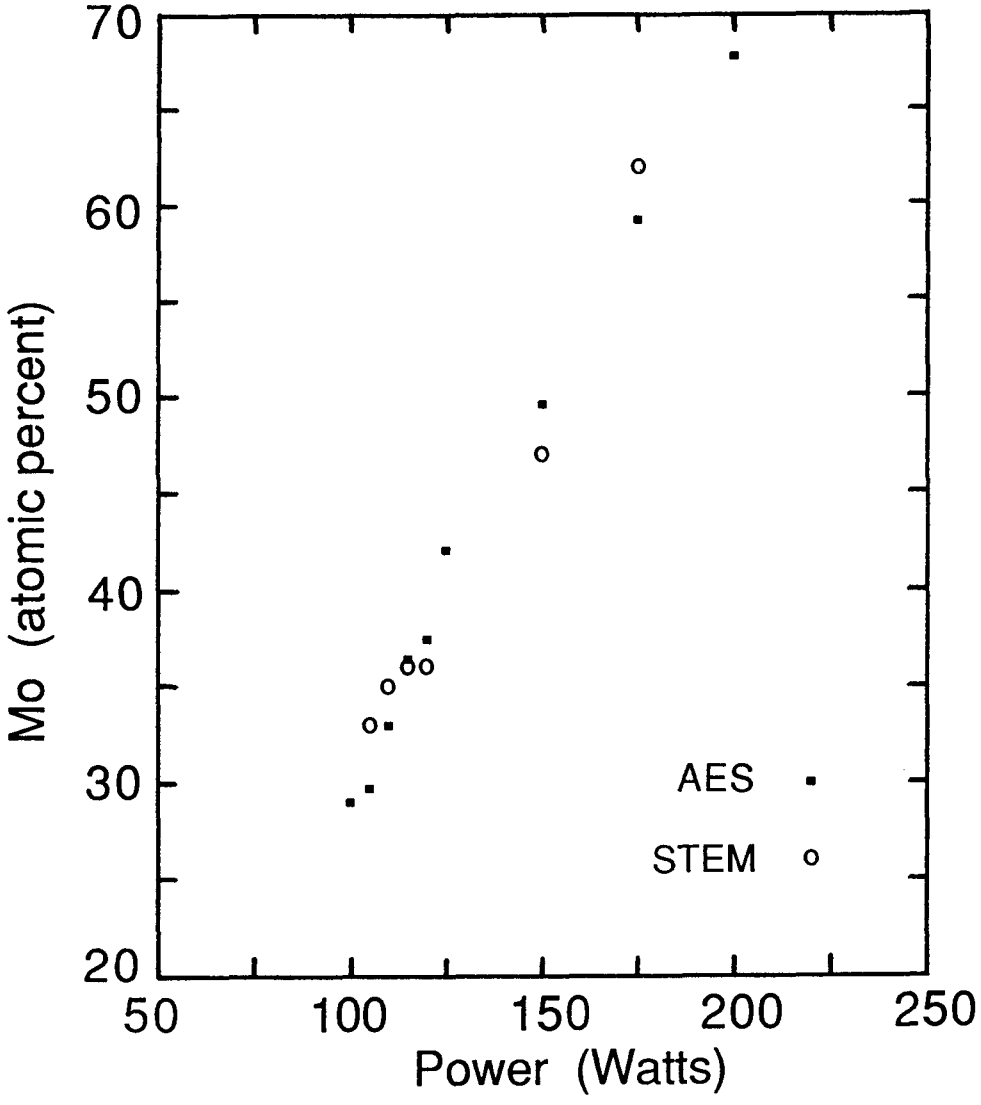
70
60
50
40
30
20
Mo (atomic percent)
50
100
150
200
250
Power (Watts)
AES
STEM

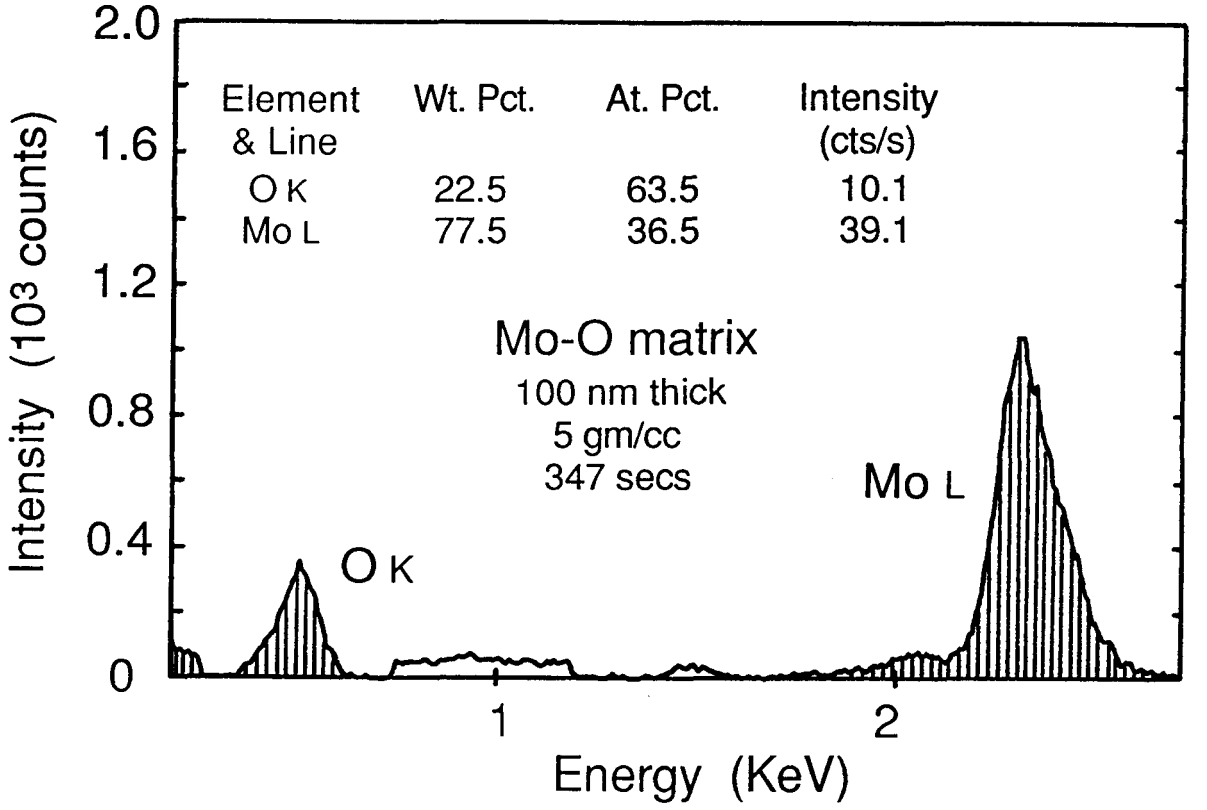
Element & Line
Wt. Pct.
At. Pct.
Intensity (cts/s)
O K 22.5 63.5 10.1
Mo L 77.5 36.5 39.1
Mo-O matrix
100 nm thick
5 gm/cc
347 secs
O K
Mo L
Intensity (10³ counts)
2.0
1.6
1.2
0.8
0.4
0
1
2
Energy (KeV)

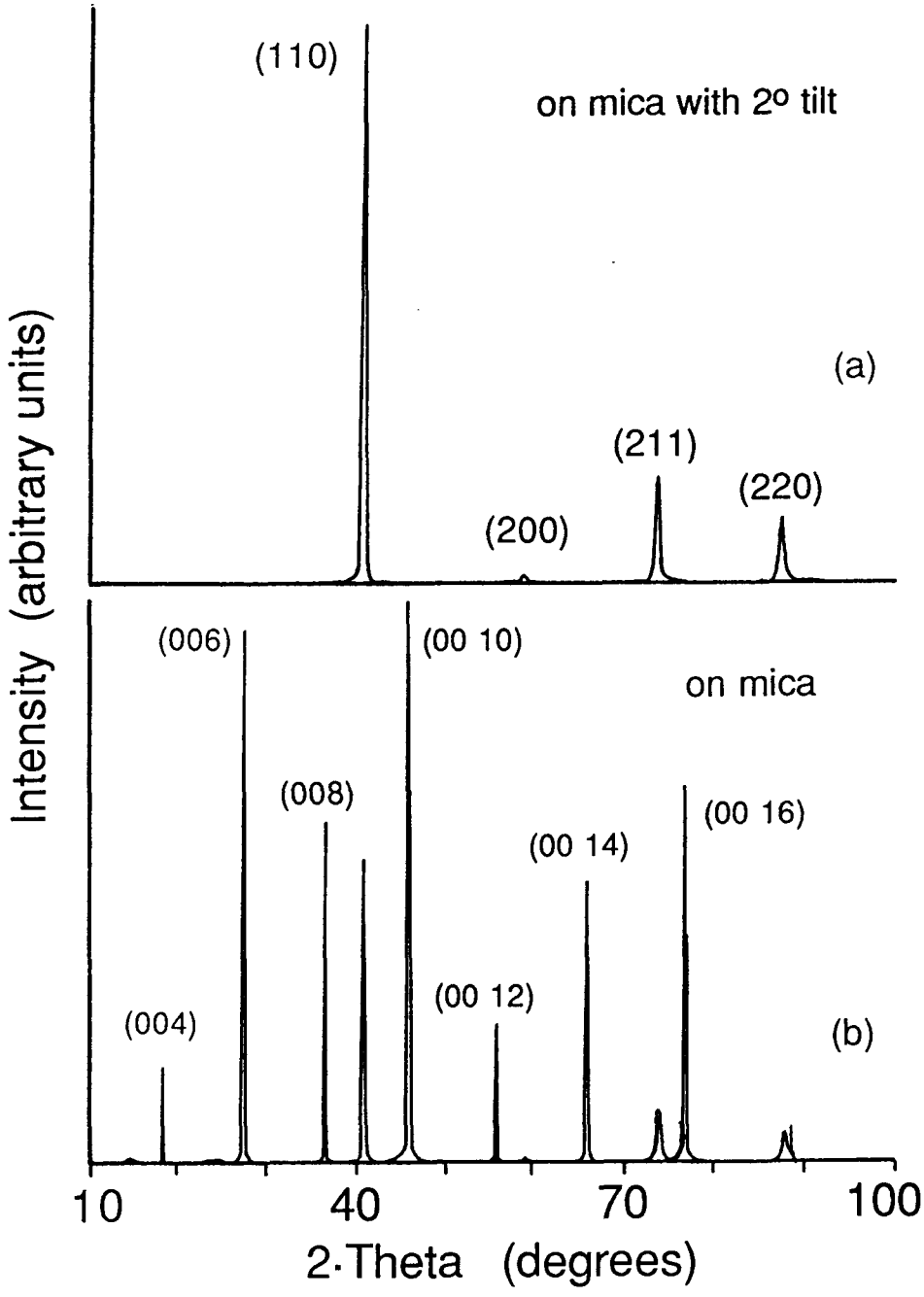
(110)
on mica with 2° tilt
(a)
(211)
(220)
(200)
(006)
(00 10)
on mica
(008)
(00 16)
(00 14)
(00 12)
(004)
(b)
Intensity (arbitrary units)
10
40
70
100
2-Theta (degrees)

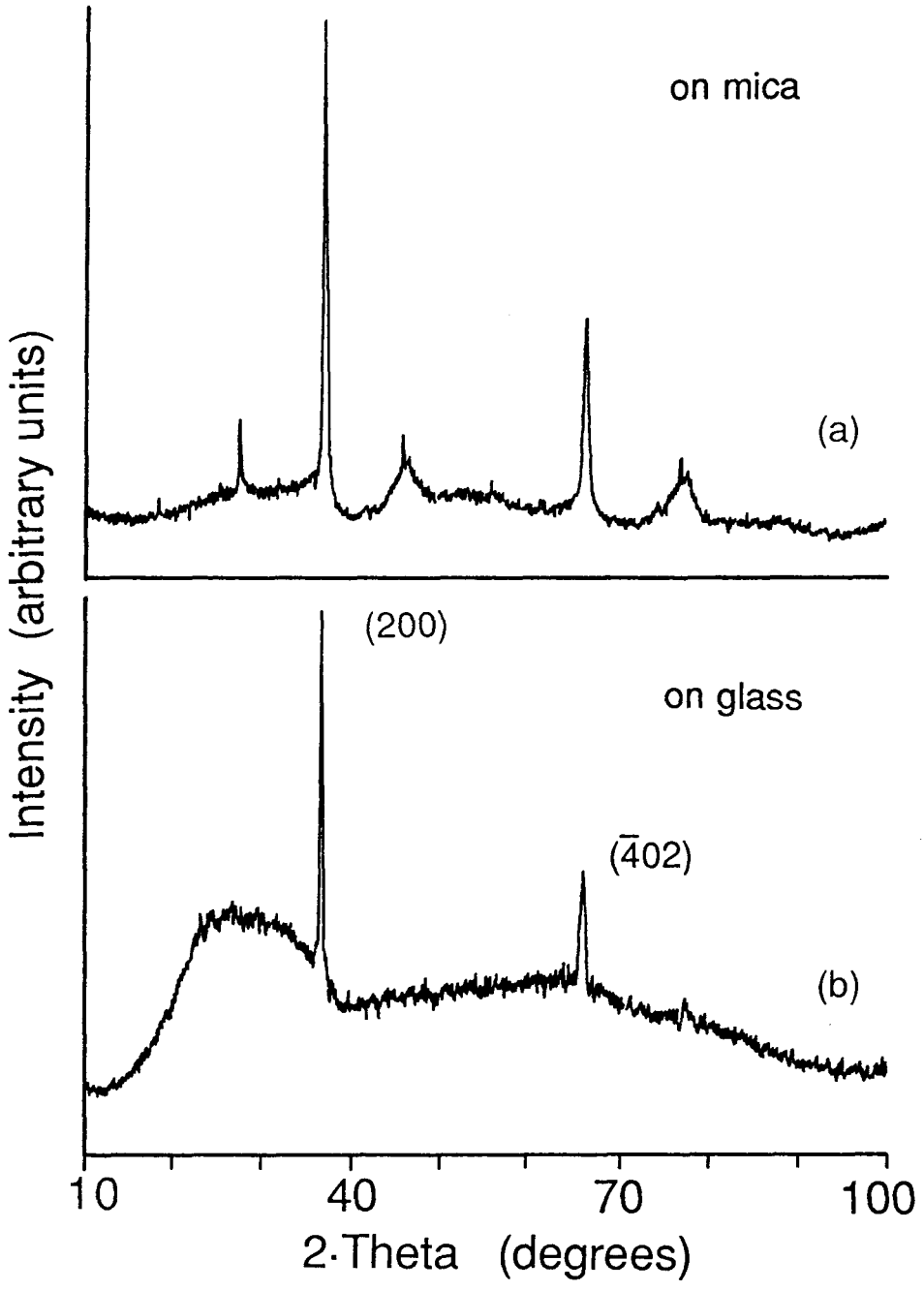
on mica
(a)
(200)
on glass
(4̄02)
(b)
Intensity (arbitrary units)
10
40
70
100
2·Theta (degrees)

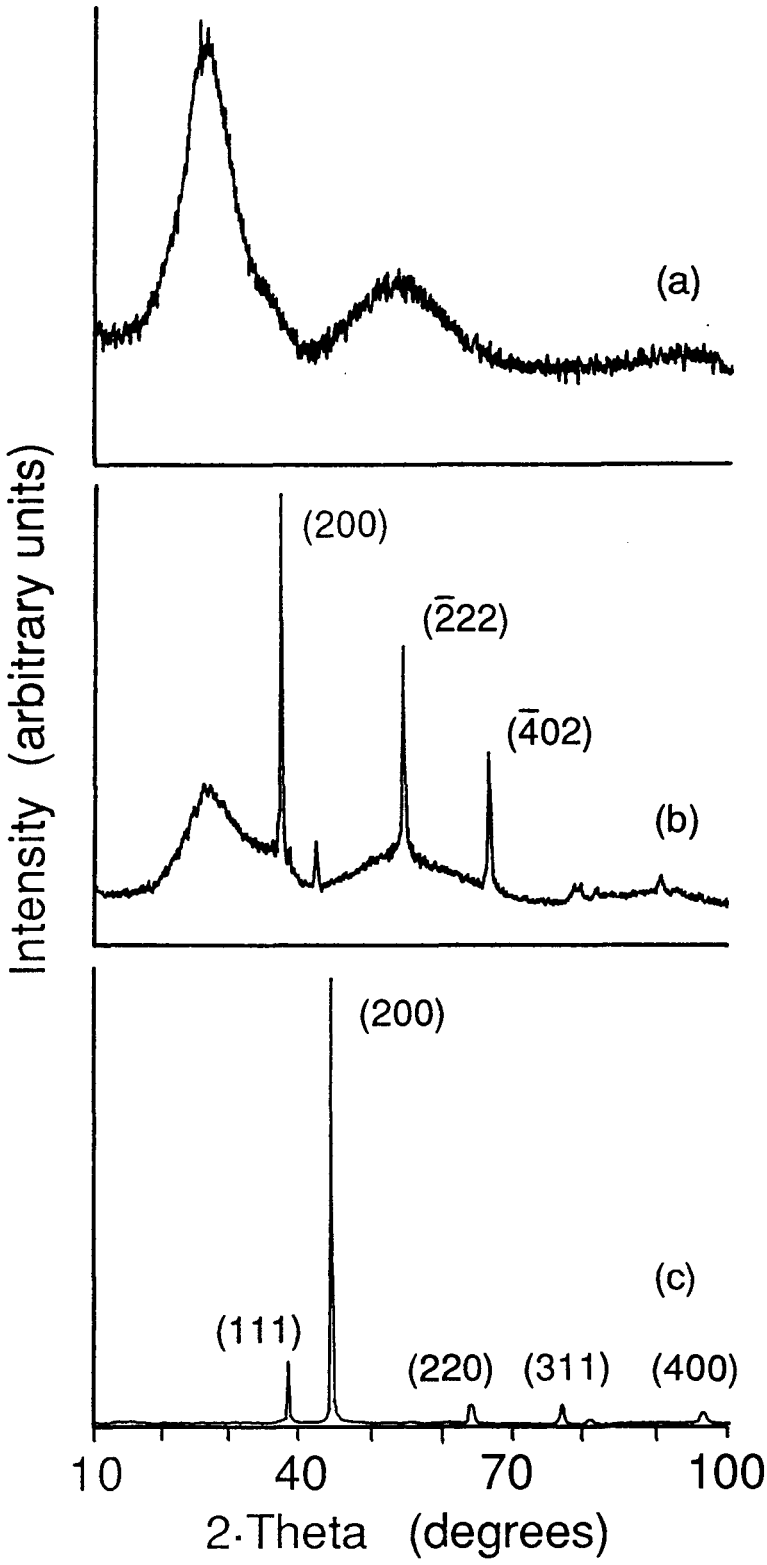
(a)
(200)
(222)
(402)
(b)
(200)
(c)
(111)
(220)
(311)
(400)
Intensity (arbitrary units)
10
40
70
100
2·Theta (degrees)

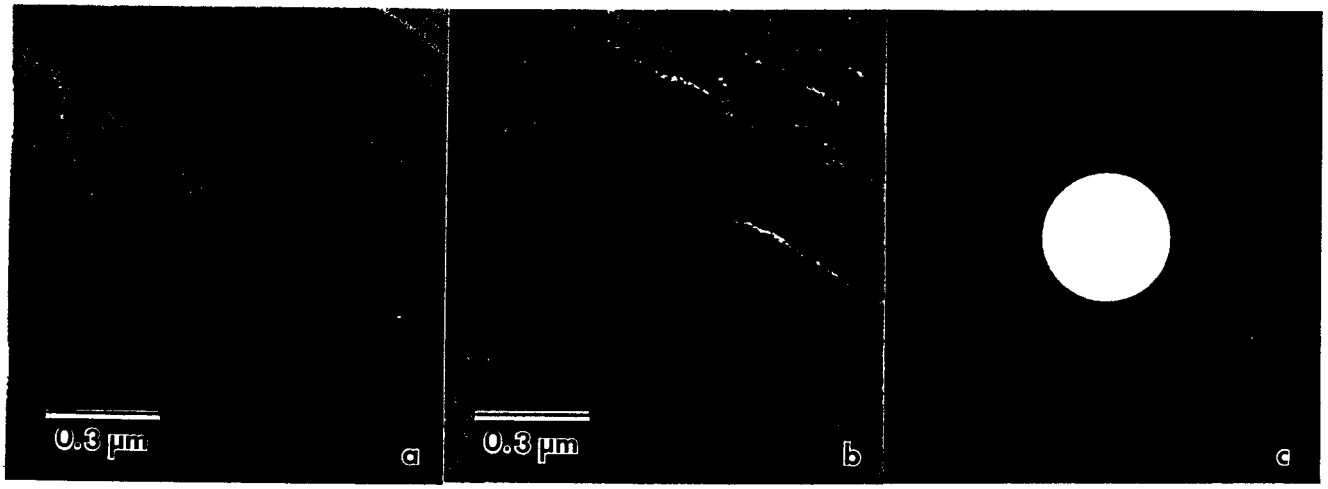
0.3 μm
a
0.3 μm
b
c

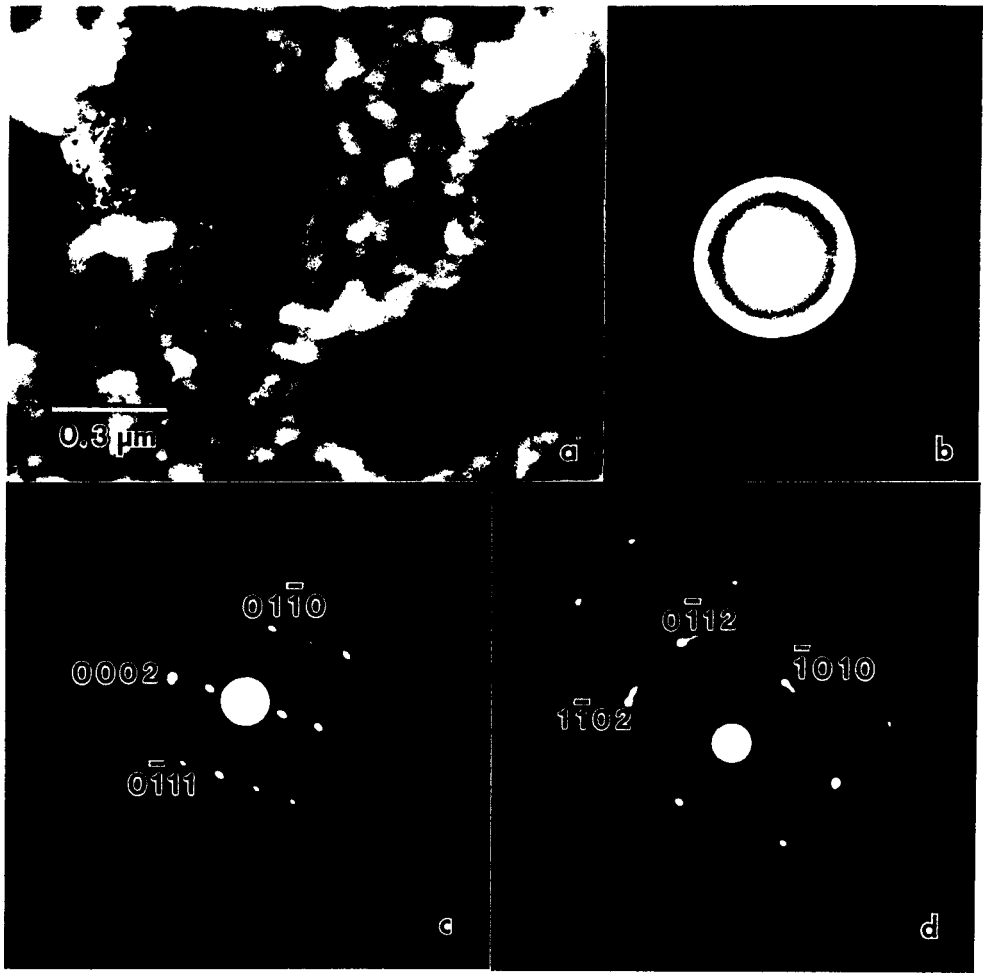
0.3 μm
a
b
0$\bar{1}$10
0002
0$\bar{1}$11
c
0$\bar{1}$12
$\bar{1}$010
1$\bar{1}$02
d

Reactive Sputtering of Molybdenum

Dr. Alan Jankowski
Lawrence Livermore National Laboratory
P. O. Box 808, L-350
Livermore, California 94550
(415) 423-2519
FAX: (415) 423-7040